

Impact of dimension-eight SMEFT operators in the electroweak precision observables and triple gauge couplings analysis in universal SMEFT

Tyler Corbett^{1,*}, Jay Desai^{2,†}, O. J. P. Éboli^{3,4,‡}, M. C. Gonzalez-Garcia^{2,4,5,§},
Matheus Martinez^{3,||} and Peter Reimitz^{3,6,¶}

¹*Faculty of Physics, University of Vienna, Boltzmanngasse 5, A-1090 Wien, Austria*

²*C. N. Yang Institute for Theoretical Physics, Stony Brook University,
Stony Brook, New York 11794-3849, USA*

³*Instituto de Física, Universidade de São Paulo, São Paulo - SP 05508-090, Brazil*

⁴*Departament de Física Quàntica i Astrofísica and Institut de Ciències del Cosmos,
Universitat de Barcelona, Diagonal 647, E-08028 Barcelona, Spain*

⁵*Institució Catalana de Recerca i Estudis Avançats (ICREA),
Passeig de Lluís Companys 23, 08010 Barcelona, Spain*

⁶*Particle Theory Department, Fermilab, P.O. Box 500, Batavia, Illinois 60510, USA*



(Received 17 April 2023; accepted 24 May 2023; published 9 June 2023)

We perform a complete study of the electroweak precision observables and electroweak gauge boson pair production in terms of the Standard Model effective field theory up to $\mathcal{O}(1/\Lambda^4)$ under the assumption of universal C and P conserving new physics. We show that the analysis of data from those two sectors allows us to obtain closed constraints in the relevant parameter space in this scenario. In particular, we find that the Large Hadron Collider data can independently constrain the Wilson coefficients of the dimension-six and -eight operators directly contributing to the triple gauge boson vertices. Our results show that the impact of dimension-eight operators in the study of triple gauge couplings is small.

DOI: [10.1103/PhysRevD.107.115013](https://doi.org/10.1103/PhysRevD.107.115013)

I. INTRODUCTION

During the last decade, the Large Hadron Collider (LHC) has accumulated a large amount of data that has led to further tests of the Standard Model (SM) and the search for physics beyond the Standard Model (BSM). Presently, there is no smoking gun indication of any extension of the SM. Therefore, one can assume that there is a mass gap between the electroweak scale and the BSM scale. In this scenario, the use of effective field theory (EFT) [1–3] as the tool to search for hints of new physics has become customary.

The EFT approach is suited for model-independent analyses since it is based exclusively on the low-energy accessible states and symmetries. Assuming that the scalar particle observed in 2012 [4,5] belongs to an electroweak

doublet, we can realize the $SU(2)_L \otimes U(1)_Y$ symmetry linearly. The resulting model is the so-called Standard Model EFT (SMEFT). There have been many analyses of the LHC data using dimension-six SMEFT; see, for instance, [6–19] and references therein. In order to assess the importance of the different contributions in the $1/\Lambda$ expansion, as well as avoid the appearance of phase space regions where the cross section is negative [11], it is important to perform the full calculation at order $1/\Lambda^4$. The consistent calculation at order $1/\Lambda^4$ requires the introduction of the contributions stemming from dimension-eight operators. In the most general scenario, the number of dimension-eight operators contributing to the present observables is extremely large [20] and that precludes a complete general analysis including all effects up to order $1/\Lambda^4$. Because of its complexity, the systematic study of the $\mathcal{O}(1/\Lambda^4)$ effects is still in its early stages. To date there have been a few case studies for Drell-Yan data [21–25], $t\bar{t}H$ production [26], the production of electroweak gauge boson pairs [27], Higgs boson processes [28–32], and electroweak precision data [32,33]. Two complete dimension-eight bases of operators for the SMEFT have been constructed in [34,35].

With this motivation, we perform a complete study of the electroweak precision observables (EWPOs) and electroweak diboson (EWDB) production at order $1/\Lambda^4$ including all relevant dimension-six and dimension-eight operators

*corbett.t.s@gmail.com

†jay.desai@stonybrook.edu

‡eboli@if.usp.br

§maria.gonzalez-garcia@stonybrook.edu

||matheus.martines.silva@usp.br

¶peter@if.usp.br

Published by the American Physical Society under the terms of the [Creative Commons Attribution 4.0 International license](https://creativecommons.org/licenses/by/4.0/). Further distribution of this work must maintain attribution to the author(s) and the published article's title, journal citation, and DOI. Funded by SCOAP³.

under the assumption of universal new physics with conservation of C and P [36], so that the EFT contains only bosonic operators after field redefinitions. In this case, we show that the analysis of existing data from those two sectors allows one to obtain closed constraints on the full relevant parameter space. Furthermore, we argue that it is still possible to perform the analysis sequentially, obtaining first the constraints on four effective combinations of Wilson coefficients using the EWPOs, and then apply those bounds to reduce the number of Wilson coefficients that are relevant for the diboson analysis.¹ In addition to demonstrating the feasibility of the analysis and deriving the corresponding bounds, our main result is to show that in this scenario the impact of dimension-eight operators in our present determination of the triple gauge couplings (TGCs) is small.

This work is organized as follows. The analysis framework employed is presented in Sec. II. Sections III and IV contain the results of the analysis of EWPO and EWDB data, respectively. In Sec. V, we summarize our conclusions. We present in the Appendixes the full expressions of

the couplings of the electroweak gauge bosons to fermions and TGCs to order $\mathcal{O}(1/\Lambda^4)$ in this scenario.

II. ANALYSIS FRAMEWORK

Following [36], we consider a theory as universal if its EFT can be expressed exclusively in terms of bosonic operators via field redefinitions. We will also assume conservation of C and P . The requirement of the EFT to be universal limits the number of operators that have to be considered, and in Ref. [36] the independent set of dimension-six operators for universal theories is explicitly worked out in several bases. In this work, we use the Hagiwara-Ishihara-Szalapski-Zeppenfeld (HISZ) dimension-six basis [37,38]. The relevant set of operators left in HISZ basis for universal theories can be straightforwardly adapted from the results in Ref. [36] for the strongly interacting light higgs (SILH) basis [39], taking into account the different choice of two of the bosonic operators left in the basis. With this, one finds that in the HISZ basis universal theories are described by 11 bosonic operators and 5 fermionic operators. The 11 bosonic operators are as follows:

$$\begin{aligned} \mathcal{O}_{\Phi,1} &= (D_\mu \Phi)^\dagger \Phi \Phi^\dagger (D^\mu \Phi), & \mathcal{O}_{\Phi,2} &= \frac{1}{2} \partial^\mu (\Phi^\dagger \Phi) \partial_\mu (\Phi^\dagger \Phi), & \mathcal{O}_{\Phi^6} &= (\Phi^\dagger \Phi)^3, \\ \mathcal{O}_{WW} &= \Phi^\dagger \hat{W}_{\mu\nu} \hat{W}^{\mu\nu} \Phi, & \mathcal{O}_{BB} &= \Phi^\dagger \hat{B}_{\mu\nu} \hat{B}^{\mu\nu} \Phi, & \mathcal{O}_{BW} &= \Phi^\dagger \hat{B}_{\mu\nu} \hat{W}^{\mu\nu} \Phi, \\ \mathcal{O}_W &= (D_\mu \Phi)^\dagger \hat{W}^{\mu\nu} (D_\nu \Phi), & \mathcal{O}_B &= (D_\mu \Phi)^\dagger \hat{B}^{\mu\nu} (D_\nu \Phi), & \mathcal{O}_{WWW} &= \text{Tr}[\hat{W}_\mu^\nu \hat{W}_\nu^\rho \hat{W}_\rho^\mu], \\ \mathcal{O}_{GG} &= \Phi^\dagger \Phi G_{\mu\nu}^a G^{a\mu\nu}, & \mathcal{O}_{GGG} &= g_s^3 f^{abc} G_{\mu\nu}^a G_\nu^{b\rho} G_\rho^{c\mu}, \end{aligned} \quad (2.1)$$

where Φ stands for the SM Higgs doublet and we have defined $\hat{B}_{\mu\nu} \equiv i(g'/2)B_{\mu\nu}$ and $\hat{W}_{\mu\nu} \equiv i(g/2)\sigma^a W_{\mu\nu}^a$, with g_s , g , and g' being the $SU(3)_C$, $SU(2)_L$, and $U(1)_Y$ gauge couplings, respectively. σ^a stands for the Pauli matrices, whereas f^{abc} are the $SU(3)_C$ structure constants.

Five four-fermion operators are generated when applying the equations of motion (EOM) to eliminate bosonic operators involving the square of derivatives of the gauge strength tensors and four Higgs fields in total analogy with the SILH basis in Ref. [36],

$$\begin{aligned} \mathcal{O}_y &= |\Phi|^2 (\Phi_a J_y^a + \text{H.c.}), & \mathcal{O}_{2y} &= J_{y\alpha}^\dagger J_y^\alpha, \\ \mathcal{O}_{2JW} &= \sum_{f,f' \in \{Q,L\}} \left(\bar{f} \gamma_\mu \frac{\sigma^a}{2} f \right) \left(\bar{f}' \gamma^\mu \frac{\sigma^a}{2} f' \right), \\ \mathcal{O}_{2JB} &= \sum_{f,f' \in \{Q,L,u,d,e\}} (Y_f \bar{f} \gamma_\mu f) (Y_{f'} \bar{f}' \gamma^\mu f'), \\ \mathcal{O}_{2JG} &= \sum_{f,f' \in \{Q,u,d\}} (\bar{f} \gamma_\mu T^a f) (\bar{f}' \gamma^\mu T^a f'), \end{aligned} \quad (2.2)$$

¹One could perform the fit for both analyses simultaneously and find the same results. However, it is numerically much simpler to perform them sequentially as is done in our analysis.

where Y_f are the hypercharges, Q and L are the quark and lepton doublets, and u , d , and e represent the fermion singlets. In addition, T^a are the Gell-Mann matrices, y_f are the Yukawa matrices, and

$$J_y^\alpha = \bar{u} y_u^\dagger Q_\beta \epsilon^{\alpha\beta} + \bar{Q}^\alpha y_d d + \bar{L}^\alpha y_e e.$$

For the dimension-eight operators, we will work in the basis defined in Ref. [34]. For universal theories, the potentially relevant bosonic operators for our analyses belong to the classes $\Phi^6 D^2$, $X^3 \Phi^2$, $X^2 \Phi^4$, and $X \Phi^4 D^2$ with X standing for a field strength tensor. This includes the following:

- (i) two operators in the class $\Phi^6 D^2$ related to the dimension-six $\mathcal{O}_{\Phi,1}$ and $\mathcal{O}_{\Phi,2}$,

$$\begin{aligned} \mathcal{O}_{D^2\Phi^6}^{(1)} &= (\Phi^\dagger \Phi)^2 (D_\mu \Phi)^\dagger D^\mu \Phi \quad \text{and} \\ \mathcal{O}_{D^2\Phi^6}^{(2)} &= (\Phi^\dagger \Phi) (\Phi^\dagger \sigma^I \Phi) (D_\mu \Phi)^\dagger \sigma^I D^\mu \Phi, \end{aligned} \quad (2.3)$$

- (ii) two CP conserving operators in class $X^3 \Phi^2$ that contribute to the EWDB analysis,

$$\begin{aligned} \mathcal{O}_{W^3\Phi^2}^{(1)} &= (\Phi^\dagger \Phi) \text{Tr}[\hat{W}_\nu^\mu \hat{W}_\rho^\nu \hat{W}_\mu^\rho] \quad \text{and} \\ \mathcal{O}_{W^2B\Phi^2}^{(1)} &= \frac{g^3 s_W}{8 c_W} \epsilon^{IJK} \Phi^\dagger \sigma^I \Phi B_\nu^\mu W_\rho^{J\nu} W_\mu^{K\rho}, \end{aligned} \quad (2.4)$$

- (iii) two operators in class $X\Phi^4 D^2$ contributing to anomalous TGCs are siblings of dimension-six operators \mathcal{O}_B and \mathcal{O}_W ,

$$\begin{aligned}\mathcal{O}_{B\Phi^4 D^2}^{(1)} &= (\Phi^\dagger \Phi)(D_\mu \Phi)^\dagger \hat{B}^{\mu\nu} D_\nu \Phi \quad \text{and} \\ \mathcal{O}_{W\Phi^4 D^2}^{(1)} &= (\Phi^\dagger \Phi)(D_\mu \Phi)^\dagger \hat{W}^{\mu\nu} D_\nu \Phi,\end{aligned}\quad (2.5)$$

- (iv) four operators in the $X^2\Phi^4$ class,

$$\begin{aligned}\mathcal{O}_{W^2\Phi^4}^{(1)} &= (\Phi^\dagger \Phi)\Phi^\dagger \hat{W}_{\mu\nu} \hat{W}^{\mu\nu} \Phi, \\ \mathcal{O}_{B^2\Phi^4}^{(1)} &= (\Phi^\dagger \Phi)^2 \hat{B}_{\mu\nu} \hat{B}^{\mu\nu},\end{aligned}\quad (2.6)$$

$$\begin{aligned}\mathcal{O}_{BW\Phi^4}^{(1)} &= (\Phi^\dagger \Phi)\Phi^\dagger \hat{W}_{\mu\nu} \Phi \hat{B}^{\mu\nu}, \\ \mathcal{O}_{W^2\Phi^4}^{(3)} &= \Phi^\dagger \hat{W}_{\mu\nu} \Phi \Phi^\dagger \hat{W}^{\mu\nu} \Phi.\end{aligned}\quad (2.7)$$

In addition, some dimension-eight fermionic operators will be generated by the EOM in analogy to the dimension-six case. Presently, there is no study of the fermionic operators compatible with universal theories for the dimension-eight basis. So in what follows, we assume that only four-fermion operators are generated in exchanging a subset of the purely bosonic operators defining the universal basis for fermionic operators.

It is important to notice that not all operators listed above appear in the analysis of EWPO and EWDB data even after accounting for their finite renormalization contribution to the SM parameters. In this work, we adopt as input parameters $\{\hat{\alpha}_{\text{em}}, \hat{G}_F, \hat{M}_Z\}$ and consider the following three relations to define the renormalized parameters:

$$\begin{aligned}\hat{e} &= \sqrt{4\pi\hat{\alpha}_{\text{em}}}, \\ \hat{v}^2 &= \frac{1}{\sqrt{2}\hat{G}_F}, \\ \hat{c}^2\hat{s}^2 &= \frac{\pi\hat{\alpha}_{\text{em}}}{\sqrt{2}\hat{G}_F\hat{M}_Z^2},\end{aligned}\quad (2.8)$$

where \hat{s} (\hat{c}) is the sine (cosine) of the weak mixing angle $\hat{\theta}$.

The predictions of SMEFT at order $1/\Lambda^4$ and the input parameters in Eq. (2.8) allow us to obtain the SM mixing angle, electric charge, and the Higgs vacuum expectation value VEV as a function of the input parameters and some of dimension-six and -eight Wilson coefficients. In this process, the operators \mathcal{O}_{WW} , \mathcal{O}_{BB} , $\mathcal{O}_{W^2\Phi^4}^{(1)}$, and $\mathcal{O}_{B^2\Phi^4}^{(1)}$ induce an overall renormalization of the W^a and B field wave functions that can be absorbed by a redefinition of the coupling constants. Furthermore, the contribution of $\mathcal{O}_{D^2\Phi^6}^{(1)}$ to the Higgs VEV cancels against its contribution to the renormalization of the W^a and B field wave functions. Consequently, their coefficients drop out of any of the

predictions in the EWPO and EWDB data (see the Appendixes for the explicit expressions).

Altogether, the effective Lagrangian considered in this work reads

$$\begin{aligned}\mathcal{L}_{\text{eff}} &= \mathcal{L}_{\text{SM}} + \frac{f_{WWW}}{\Lambda^2} \mathcal{O}_{WWW} + \frac{f_W}{\Lambda^2} \mathcal{O}_W + \frac{f_B}{\Lambda^2} \mathcal{O}_B \\ &+ \frac{f_{BW}}{\Lambda^2} \mathcal{O}_{BW} + \frac{f_{\Phi,1}}{\Lambda^2} \mathcal{O}_{\Phi,1} + \frac{f_{4F}}{\Lambda^2} \mathcal{O}_{4F} + \frac{f_{D^2\Phi^6}^{(2)}}{\Lambda^4} \mathcal{O}_{D^2\Phi^6}^{(2)} \\ &+ \frac{f_{W^3\Phi^2}^{(1)}}{\Lambda^4} \mathcal{O}_{W^3\Phi^2}^{(1)} + \frac{f_{W^2B\Phi^2}^{(1)}}{\Lambda^4} \mathcal{O}_{W^2B\Phi^2}^{(1)} + \frac{f_{B\Phi^4 D^2}^{(1)}}{\Lambda^4} \mathcal{O}_{B\Phi^4 D^2}^{(1)} \\ &+ \frac{f_{W\Phi^4 D^2}^{(1)}}{\Lambda^4} \mathcal{O}_{W\Phi^4 D^2}^{(1)} + \frac{f_{W^2\Phi^4}^{(3)}}{\Lambda^4} \mathcal{O}_{W^2\Phi^4}^{(3)} \\ &+ \frac{f_{BW\Phi^4}^{(1)}}{\Lambda^4} \mathcal{O}_{BW\Phi^4}^{(1)} + \frac{f_{4F}^{(8)}}{\Lambda^4} \mathcal{O}_{4F}^{(8)},\end{aligned}\quad (2.9)$$

where \mathcal{O}_{4F} stands for the part of \mathcal{O}_{2JW} that contributes to the muon decay, whereas $\mathcal{O}_{4F}^{(8)}$ is the corresponding dimension-eight operator. They have been defined so that their contribution to the Higgs field vacuum expectation value in the SM Lagrangian reads

$$\left[2\langle\Phi^\dagger\Phi\rangle - \frac{1}{\sqrt{2}\hat{G}_F}\right]_{\text{fermionic}} \equiv \frac{\hat{v}^4}{\Lambda^2} \Delta_{4F} + \frac{\hat{v}^6}{\Lambda^4} \Delta_{4F}^{(8)}. \quad (2.10)$$

Defined in this way, Δ_{4F} is the dimension-six correction proportional to f_{4F} and $\Delta_{4F}^{(8)}$ contains the linear correction from $f_{4F}^{(8)}$ as well as one term proportional to $(f_{4F})^2$ [32,33].²

The predictions for observables at order $1/\Lambda^4$ require evaluating the SM contributions, the interference between the $1/\Lambda^2$ amplitude ($\mathcal{M}^{(6)}$) with the SM amplitude, and the square of the dimension-six amplitude, as well as the interference of the dimension-eight amplitude $\mathcal{M}^{(8)}$ with the SM one, which we represent as

$$|\mathcal{M}_{\text{SM}}|^2 + \mathcal{M}_{\text{SM}}^* \mathcal{M}^{(6)} + |\mathcal{M}^{(6)}|^2 + \mathcal{M}_{\text{SM}}^* \mathcal{M}^{(8)}. \quad (2.11)$$

Notice that $\mathcal{M}^{(8)}$ includes dimension-eight vertices as well as the contribution of the insertion of two dimension-six couplings in the amplitude.

²We introduce the subscript “fermionic” in Eq. (2.10) because at dimension-eight the bosonic operators $\mathcal{O}_{D^2\Phi^6}^{(1)}$ and $\mathcal{O}_{D^2\Phi^6}^{(2)}$ also contribute to $\langle\Phi^\dagger\Phi\rangle - \hat{v}^2$. The corrections from $\mathcal{O}_{D^2\Phi^6}^{(1)}$ cancel in the final expressions of the observables, whereas those from $\mathcal{O}_{D^2\Phi^6}^{(2)}$ are kept separately to be combined with the corrections from that operator to the other SM parameters in the final expression of the observables.

III. EWPO ANALYSIS

Our EWPO analysis includes 14 observables, of which 12 are Z observables [40],

$$\Gamma_Z, \quad \sigma_h^0, \quad \mathcal{A}_\ell(\tau^{\text{pol}}), \quad R_\ell^0, \quad \mathcal{A}_\ell(\text{SLD}), \quad A_{\text{FB}}^{0,l}, \\ R_c^0, \quad R_b^0, \quad \mathcal{A}_c, \quad \mathcal{A}_b, \quad A_{\text{FB}}^{0,c}, \quad \text{and } A_{\text{FB}}^{0,b} \text{ (SLD/LEP-I),}$$

supplemented by two W observables

$$M_W, \quad \Gamma_W$$

that are, respectively, its average W -boson mass taken from [41]³ and its width from LEP2/Tevatron [43].⁴ The correlations among these inputs [40] are taken into consideration in the analyses. The SM predictions and their uncertainties due to variations of the SM parameters were extracted from [44].

The statistical analysis of the EWPO data is made by means of a binned log-likelihood function defining a χ^2 function that depends on seven Wilson coefficients,

$$\chi_{\text{EWPO}}^2 \equiv \chi_{\text{EWPO}}^2 \left(f_{BW}, f_{\Phi,1}, \Delta_{4F}, f_{BW\Phi^4}^{(1)}, f_{D^2\Phi^6}^{(2)}, \Delta_{4F}^{(8)}, f_{W^2\Phi^4}^{(3)} \right). \quad (3.1)$$

In fact, EWPOs cannot constrain the seven Wilson coefficients independently. This is so because, as described in Appendix A, the corrections to the Z interaction to fermions to order Λ^{-4} can be expressed in terms of the following three combinations of Wilson coefficients:

$$\begin{aligned} \tilde{\Delta}_{4F} &= \Delta_{4F} + \frac{\hat{v}^2}{\Lambda^2} \Delta_{4F}^{(8)}, \\ \tilde{f}_{BW} &= f_{BW} + \frac{\hat{v}^2}{2\Lambda^2} f_{BW\Phi^4}^{(1)}, \\ \tilde{f}_{\Phi,1} &= f_{\Phi,1} + \frac{\hat{v}^2}{\Lambda^2} f_{D^2\Phi^6}^{(2)}. \end{aligned} \quad (3.2)$$

The corrections to the W mass and coupling to fermions further involve the addition of only one operator $\mathcal{O}_{W^2\Phi^4}^{(3)}$. Using these variables, we incorporate in our calculation some higher order terms in the $1/\Lambda$ expansion in the spirit of geometric SMEFT [33,45].

These three coefficient combinations and $f_{W^2\Phi^4}^{(3)}$ are directly related to the contributions to the oblique S , T , U parameters [46] and δG_F [32,33] at linear order in Wilson coefficients of operators up to dimension-eight,

$$\begin{aligned} \alpha S &= -\hat{e}^2 \frac{\hat{v}^2}{\Lambda^2} \tilde{f}_{BW}, & \alpha T &= -\frac{\hat{v}^2}{2\Lambda^2} \tilde{f}_{\Phi,1}, \\ \alpha U &= \hat{e}^2 \frac{\hat{v}^4}{\Lambda^4} f_{W^2\Phi^4}^{(3)}, & \frac{\delta G_F}{\hat{G}_F} &= \frac{\hat{v}^2}{\Lambda^2} \tilde{\Delta}_{4F}. \end{aligned} \quad (3.3)$$

It is interesting to notice that there is a contribution to the oblique parameter U at dimension eight. Thus, effectively the EWPO chi-squared function is

$$\tilde{\chi}_{\text{EWPO}}^2 \equiv \chi_{\text{EWPO}}^2(\tilde{f}_{BW}, \tilde{f}_{\Phi,1}, f_{W^2\Phi^4}^{(3)}, \tilde{\Delta}_{4F}). \quad (3.4)$$

Figure 1 shows the one- and two-dimensional projections of $\Delta\tilde{\chi}_{\text{EWPO}}^2$ as a function of the coefficients $\tilde{f}_{BW}\hat{v}^2/\Lambda^2$, $\tilde{f}_{\Phi,1}\hat{v}^2/\Lambda^2$, $\delta G_F/\hat{G}_F$, and $f_{W^2\Phi^4}^{(3)}\hat{v}^4/\Lambda^4$. The panels in the top row contain the one-dimension marginalized projection of $\Delta\tilde{\chi}_{\text{EWPO}}^2$, where the dashed line stands for the $\mathcal{O}(1/\Lambda^2)$ analysis, whereas the green solid one also contains the dimension-six-squared contribution. The full analysis that includes the dimension-eight contribution is represented by the blue line. As seen in the figure, the results at linear dimension-six and dimension-six squared are identical, which is expected given the precision of the data.

From Fig. 1 we also see that once the dimension-eight coefficient $f_{W^2\Phi^4}^{(3)}$ is included the bounds on $\tilde{f}_{\Phi,1}\hat{v}^2/\Lambda^2$ and $\delta G_F/\hat{G}_F$ weaken by about a factor of 10. The main reason is that when $f_{W^2\Phi^4}^{(3)}$ is also included in the analysis cancellations can occur. In particular, as can be seen in Eqs. (A2)–(A4) for

$$\tilde{f}_{\Phi,1} = -2\tilde{\Delta}_{4F} = \frac{\hat{e}^2}{2\hat{s}^2} \frac{\hat{v}^2}{\Lambda^2} f_{W^2\Phi^4}^{(3)}, \quad (3.5)$$

the linear contributions from $\tilde{f}_{\Phi,1}$ (i.e., T), $\tilde{\Delta}_{4F}$ ($\delta G_F/\hat{G}_F$) and $f_{W^2\Phi^4}^{(3)}$ (U), cancel both in the Z observables and in M_W . Therefore, along this direction in the parameter space, the bounds on these three quantities dominantly come from the contribution of Γ_W in Eq. (A6), but this observable is less precisely determined, hence the strong correlations we observe in the corresponding two-dimensional allowed regions in Fig. 1. Nevertheless, the limits are still quite stringent; see Table I.

IV. DIBOSON ANALYSIS

The electroweak production of WZ , WW , and $W\gamma$ pairs, as well as the vector boson fusion production of Z 's (Zjj), collectively denoted by EWDB, allow us to study the triple couplings of electroweak gauge bosons. In this work, we consider the EWDB data shown in Table II, which comprise a total of 73 data points.

The theoretical predictions needed for the EWDB data are obtained by simulating at leading order the W^+W^- ,

³In order to be conservative, we did not take into account the recent CDF measurement of the W mass [42].

⁴We do not include the average leptonic W branching ratio because it does not include any additional constraint for universal EFT.

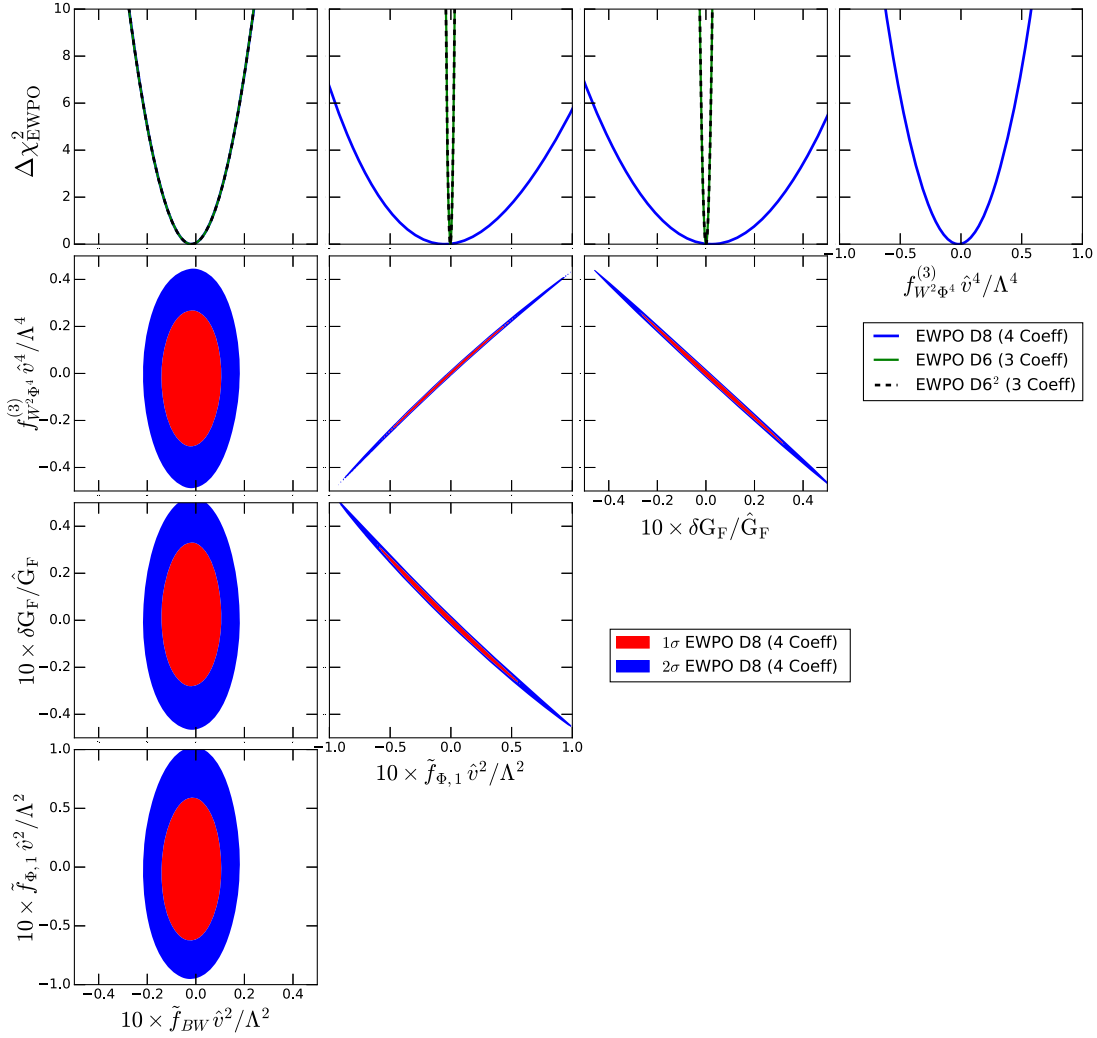


FIG. 1. One- and two-dimensional projections of $\Delta\chi^2_{\text{EWPO}}$ for the coefficients $\tilde{f}_{BW}\hat{v}^2/\Lambda^2$, $\tilde{f}_{\Phi,1}\hat{v}^2/\Lambda^2$, $\delta G_F/\hat{G}_F$, and $f_{W^2\Phi^4}^{(3)}\hat{v}^4/\Lambda^4$, as indicated in each panel after marginalizing over the undisplayed parameters.

$W^\pm Z$, $W^\pm \gamma$, and Zjj channels that receive contributions from TGCs. To this end, we use MadGraph5_aMC@NLO [54] with the UFO files for our effective Lagrangian generated with FeynRules [55,56]. We employ PYTHIA8 [57] to perform

TABLE I. 95% C.L. allowed ranges for the effective couplings entering in the EWPOs with the analysis done including only the dimension-six contributions (left column) and also the dimension-eight contributions (right column).

Coupling	EWPO 95% C.L. allowed range	
	Dimension 6	Dimension 8
$\frac{\hat{v}^2}{\Lambda^2} \tilde{f}_{BW}$	$[-0.018, 0.014]$	$[-0.018, 0.014]$
$\frac{\hat{v}^2}{\Lambda^2} \tilde{f}_{\Phi,1}$	$[-0.0028, 0.0018]$	$[-0.080, 0.081]$
$\frac{\delta G_F}{\hat{G}_F}$	$[-0.0016, 0.0017]$	$[-0.038, 0.044]$
$\frac{\hat{v}^4}{\Lambda^4} f_{W^2\Phi^4}^{(3)}$		$[-0.40, 0.36]$

the parton shower and hadronization, while the fast detector simulation is carried out with DELPHES [58]. Jet analyses are performed using FASTJET [59].

The results of the analysis can be qualitatively understood in terms of the effective $\gamma W^+ W^-$ and $Z W^+ W^-$ TGCs introduced in Ref. [60],

$$\mathcal{L}_{WWV} = -ig_{WWV} \left\{ g_1^V (W_\mu^+ W^{-\mu} V^\nu - W_\mu^+ V_\nu W^{-\mu\nu}) + \kappa_V W_\mu^+ W_\nu^- V^{\mu\nu} + \frac{\lambda_V}{\hat{M}_W^2} W_{\mu\nu}^+ W^{-\nu\rho} V_\rho^\mu \right\}, \quad (4.1)$$

where $g_{WW\gamma} = \hat{e}$, $g_{WWZ} = \hat{e} \hat{c}/\hat{s}$, and $\hat{M}_W = \hat{e} \hat{v}/2\hat{s}$. In the SM $g_1^V = g_1^Z = \kappa_\gamma = \kappa_Z = 1$ and $\lambda_Z = \lambda_\gamma = 0$. After including the direct contribution from the dimension-six and dimension-eight operators, electromagnetic gauge invariance still enforces $g_1^V = 1$, while the other effective TGCs couplings read

TABLE II. EWDB data from LHC used in the analyses. For the W^+W^- results from ATLAS run 2 [47] we combine the data from the last three bins into one to ensure Gaussianity.

	Channel (a)	Distribution	No. bins	Dataset (TeV)	Integrated Luminosity (fb $^{-1}$)
EWDB data	$WZ \rightarrow \ell^+ \ell^- \ell'^{\pm}$	$M(WZ)$	7	CMS 13	137.2 [48]
	$WW \rightarrow \ell^+ \ell'^{(\prime)-} + 0/1j$	$M(\ell^+ \ell'^{(\prime)-})$	11	CMS 13	35.9 [49]
	$W\gamma \rightarrow \ell \nu \gamma$	$\frac{d^2\sigma}{dp_T d\phi}$	12	CMS 13	137.1 [50]
	$WW \rightarrow e^{\pm} \mu^{\mp} + \cancel{E}_T(0j)$	m_T	17 (15)	ATLAS 13	36.1 [47]
	$WZ \rightarrow \ell^+ \ell^- \ell'^{(\prime)\pm}$	m_T^{WZ}	6	ATLAS 13	36.1 [51]
	$Zjj \rightarrow \ell^+ \ell^- jj$	$\frac{d\sigma}{d\phi}$	12	ATLAS 13	139 [52]
	$WW \rightarrow \ell^+ \ell'^{(\prime)-} + \cancel{E}_T(1j)$	$\frac{d\sigma}{dm_{\ell^+ \ell'^{-}}}$	10	ATLAS 13	139 [53]

$$\begin{aligned}
\Delta g_1^Z &= \frac{\hat{e}^2}{\hat{s}^2 \hat{c}^2} \left[\frac{1}{8} \frac{\hat{v}^2}{\Lambda^2} \left(f_W + \frac{\hat{v}^2}{2\Lambda^2} f_{W\Phi^4 D^2}^{(1)} \right) \right], \\
\Delta \kappa_\gamma &= \frac{\hat{e}^2}{\hat{s}^2} \left[\frac{1}{8} \frac{\hat{v}^2}{\Lambda^2} \left(f_W + \frac{\hat{v}^2}{2\Lambda^2} f_{W\Phi^4 D^2}^{(1)} + f_B + \frac{\hat{v}^2}{2\Lambda^2} f_{B\Phi^4 D^2}^{(1)} \right) \right], \\
\Delta \kappa_Z &= \frac{\hat{e}^2}{\hat{s}^2} \left[\frac{1}{8} \frac{\hat{v}^2}{\Lambda^2} \left(f_W + \frac{\hat{v}^2}{2\Lambda^2} f_{W\Phi^4 D^2}^{(1)} \right) - \frac{\hat{s}^2}{8\hat{c}^2} \frac{\hat{v}^2}{\Lambda^2} \left(f_B + \frac{\hat{v}^2}{2\Lambda^2} f_{B\Phi^4 D^2}^{(1)} \right) \right], \\
\lambda_\gamma &= \frac{3\hat{e}^2}{2\hat{s}^2} \frac{\hat{M}_W^2}{\Lambda^2} \left[f_{WWW} + \frac{\hat{v}^2}{2\Lambda^2} f_{W^3\Phi^2}^{(1)} \right] - \frac{\hat{M}_W^4}{2\Lambda^4} f_{W^2 B\Phi^2}^{(1)}, \\
\lambda_Z &= \frac{3\hat{e}^2}{2\hat{s}^2} \frac{\hat{M}_W^2}{\Lambda^2} \left[f_{WWW} + \frac{\hat{v}^2}{2\Lambda^2} f_{W^3\Phi^2}^{(1)} \right] + \frac{\hat{M}_W^4}{2\Lambda^4} \frac{\hat{s}^2}{\hat{c}^2} f_{W^2 B\Phi^2}^{(1)}.
\end{aligned} \tag{4.2}$$

The complete analysis of diboson production at fixed order $1/\Lambda^4$ depends on not only the direct SMEFT contributions to TGCs in (4.2), but also on the indirect contributions from \mathcal{O}_{BW} , $\mathcal{O}_{\Phi,1}$, \mathcal{O}_{4F} , $\mathcal{O}_{BW\Phi^4}^{(1)}$, $\mathcal{O}_{D^2\Phi^6}^{(2)}$, and $\mathcal{O}_{4F}^{(8)}$, through renormalization of the SM gauge couplings to fermions and TGCs. In Appendix B we list the complete expressions and show that, in fact, the indirect effects involve the same three combinations (3.2) and are therefore bounded by the EWPOs. In light of the constraints derived in the previous section, in what follows we will neglect the effect of those operators in the EWDB data analysis and set the combinations in Eq. (3.2) to zero in what follows.

For the direct effects, Eq. (4.2) explicitly shows that the contributions of the dimension-eight operators $\mathcal{O}_{W\Phi^4 D^2}^{(1)}$, $\mathcal{O}_{B\Phi^4 D^2}^{(1)}$, and $\mathcal{O}_{W^3\Phi^2}^{(1)}$ to the TGCs couplings have the same structure of the contributions from the dimension-six operators \mathcal{O}_W , \mathcal{O}_B and \mathcal{O}_{WWW} , respectively. Conversely, $\mathcal{O}_{W^2 B\Phi^2}^{(1)}$ contributes a purely $\mathcal{O}(1/\Lambda^4)$ to $\lambda_\gamma \neq \lambda_Z$.

Following an approach equivalent to that employed for the analysis of EWPOs we can define three effective coefficients,

$$\begin{aligned}
\tilde{f}_W &= f_W + \frac{\hat{v}^2}{2\Lambda^2} f_{W\Phi^4 D^2}^{(1)}, \\
\tilde{f}_B &= f_B + \frac{\hat{v}^2}{2\Lambda^2} f_{B\Phi^4 D^2}^{(1)}, \\
\tilde{f}_{WWW} &= f_{WWW} + \frac{\hat{v}^2}{2} f_{W^3\Phi^2}^{(1)},
\end{aligned} \tag{4.3}$$

which, together with $f_{W^2 B\Phi^2}^{(1)}$, effectively parametrize the relevant contributions to the EWDB analysis.

Following this approach, we perform the statistical analysis of the EWDB data using a binned chi-squared function defined in terms of these effective coefficients,

$$\tilde{\chi}_{\text{EWDB}}^2 \left(\tilde{f}_W, \tilde{f}_B, \tilde{f}_{WWW}, f_{W^2 B\Phi^2}^{(1)} \right). \tag{4.4}$$

Figure 2 depicts the one- and two-dimensional marginalized 68% and 95% C.L. allowed regions for $\tilde{f}_W \hat{v}^2/\Lambda^2$, $\tilde{f}_B \hat{v}^2/\Lambda^2$, $\tilde{f}_{WWW} \hat{v}^2/\Lambda^2$, and $f_{W^2 B\Phi^2}^{(1)} \hat{v}^4/\Lambda^4$ after marginalizing over the remaining fit parameters. The light pink (blue) regions in these panels correspond to the 68% (95%) C.L. allowed regions of the $\mathcal{O}(1/\Lambda^2)$ analysis; see the three lower panels. This analysis yields the marginalized

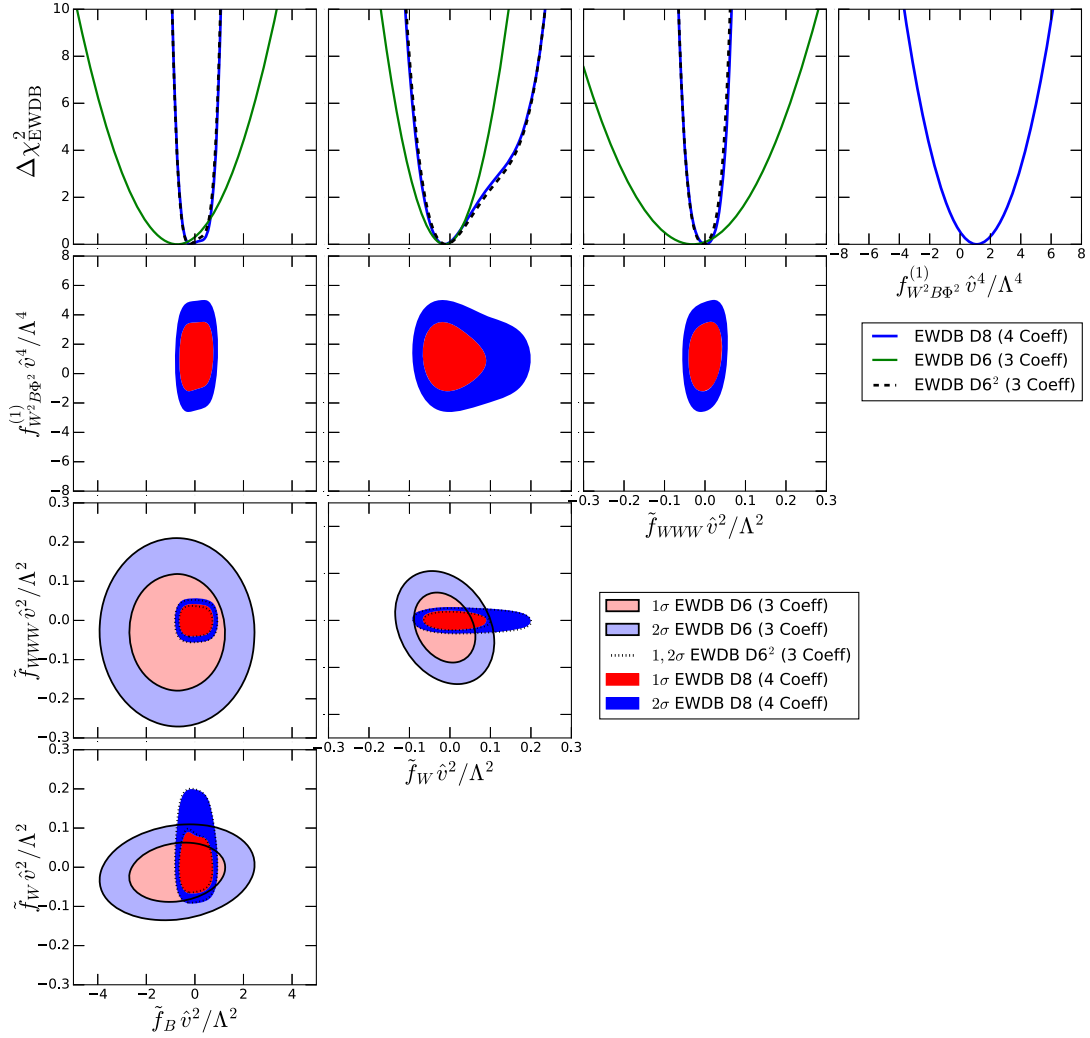


FIG. 2. One- and two-dimensional projections of $\Delta\chi^2_{\text{EWDB}}$ for the effective coefficients $\tilde{f}_W \hat{v}^2/\Lambda^2$, $\tilde{f}_B \hat{v}^2/\Lambda^2$, $\tilde{f}_{WW} \hat{v}^2/\Lambda^2$, and $f_{W^2B\Phi^2}^{(1)} \hat{v}^4/\Lambda^4$ as indicated in each panel after marginalizing over the undisplayed parameters.

95% C.L. allowed intervals for the Wilson coefficients of the three relevant dimension-six operators displayed in the left column of Table III.

TABLE III. 95% C.L. allowed ranges for the effective couplings entering in the EWDB analysis including only up to the dimension-six contributions (left column), up to the dimension-six-squared contributions (central column), and including also the dimension-eight contributions (right column).

Coupling	EWDB 95% C.L. allowed range		
	Dimension 6	(Dimension 6) ²	Dimension 8
$\frac{\hat{v}^2}{\Lambda^2} \tilde{f}_B$	$[-3.3, 1.8]$	$[-0.75, 0.83]$	$[-0.73, 0.86]$
$\frac{\hat{v}^2}{\Lambda^2} \tilde{f}_W$	$[-0.11, 0.085]$	$[-0.079, 0.16]$	$[-0.080, 0.16]$
$\frac{\hat{v}^2}{\Lambda^2} \tilde{f}_{WW}$	$[-0.22, 0.16]$	$[-0.049, 0.045]$	$[-0.048, 0.049]$
$\frac{\hat{v}^4}{\Lambda^4} f_{W^2B\Phi^2}^{(1)}$			$[-1.9, 4.2]$

The dark red (blue) shaded regions in Fig. 2 represent the two-dimensional allowed regions at 68% (95%) C.L., including also the dimension-six-squared and the dimension-eight contributions. The corresponding one-dimensional projections are given in the blue lines in the upper panels. For the sake of comparison, we also show the corresponding results including only the dimension-six-squared contributions. These are the black dashed lines in the one-dimensional projections in the upper panels and the dotted line contours in the three lower panels. From the figure we see that including the $1/\Lambda^4$ effects lead to stronger bounds on the effective coefficients \tilde{f}_B and \tilde{f}_{WW} , whereas the bound for \tilde{f}_W is slightly looser and shifted; see also the central and right columns of Table III. We traced the counterintuitive behavior of the bounds on \tilde{f}_W to the WZ datasets. Removing WZ production from the fit leads to stronger limits at the $\mathcal{O}(1/\Lambda^4)$ also for \tilde{f}_W .

The results in Fig. 2 also show that the dimension-six-squared terms are dominant over the dimension-eight one. Or, in other words, the inclusion of the relevant dimension-eight operator in this analysis, $\mathcal{O}_{W^2 B \Phi^2}^{(1)}$, has very little impact on the results. The physical reason for this can be traced to the different dependence on the partonic center-of-mass

energy (\hat{S}) of the contribution to the relevant squared amplitudes from dimension-six-squared and dimension-eight terms. As it is well known, the anomalous TGCs spoil the cancellations that take place in the SM, allowing the scattering amplitudes to grow with the partonic center-of-mass energy. The fastest growing amplitudes are (for $\hat{S} \gg m_{W,Z}$)

$$\begin{aligned}
\mathcal{M}(d_- \bar{d}_+ \rightarrow W_0^+ W_0^-) &= -i \frac{\hat{e}^2}{24 \hat{s}^2 \hat{c}^2} \frac{\hat{S}}{\Lambda^2} \sin \theta \left[3 \hat{c}^2 f_W - \hat{s}^2 f_B + \frac{\hat{v}^2}{2 \Lambda^2} \left(3 \hat{c}^2 f_{W \Phi^4 D^2}^{(1)} - \hat{s}^2 f_{B \Phi^4 D^2}^{(1)} \right) \right], \\
\mathcal{M}(d_+ \bar{d}_- \rightarrow W_\pm^+ W_\pm^-) &= i \frac{\hat{e}^2}{48 \hat{s}^2 \hat{c}^2} \frac{\hat{S}}{\Lambda^2} \sin \theta \frac{\hat{v}^2}{\Lambda^2} f_{W^2 B \Phi^2}^{(1)}, \\
\mathcal{M}(d_- \bar{d}_+ \rightarrow W_\pm^+ W_\pm^-) &= -i \frac{3 \hat{e}^4}{8 \hat{s}^4} \frac{\hat{S}}{\Lambda^2} \sin \theta \left[f_{WWW} + \frac{\hat{v}^2}{2 \Lambda^2} \left(f_{W^3 \Phi^2}^{(1)} + \frac{\hat{s}^2}{18 \hat{c}^2} f_{W^2 B \Phi^2}^{(1)} \right) \right], \\
\mathcal{M}(d_+ \bar{d}_- \rightarrow W_0^+ W_0^-) &= -i \frac{\hat{e}^2}{12 \hat{c}^2} \frac{\hat{S}}{\Lambda^2} \sin \theta \left(f_B + \frac{\hat{v}^2}{2 \Lambda^2} f_{B \Phi^4 D^2}^{(1)} \right), \\
\mathcal{M}(u_- \bar{u}_+ \rightarrow W_0^+ W_0^-) &= i \frac{\hat{e}^2}{24 \hat{s}^2 \hat{c}^2} \frac{\hat{S}}{\Lambda^2} \sin \theta \left[3 \hat{c}^2 f_W + \hat{s}^2 f_B + \frac{\hat{v}^2}{2 \Lambda^2} \left(3 \hat{c}^2 f_{W \Phi^4 D^2}^{(1)} + \hat{s}^2 f_{B \Phi^4 D^2}^{(1)} \right) \right], \\
\mathcal{M}(u_+ \bar{u}_- \rightarrow W^+ W^-) &= i \frac{\hat{e}^2}{6 \hat{c}^2} \frac{\hat{S}}{\Lambda^2} \sin \theta \left(f_B + \frac{\hat{v}^2}{2 \Lambda^2} f_{B \Phi^4 D^2}^{(1)} \right), \\
\mathcal{M}(u_+ \bar{u}_- \rightarrow W_\pm^+ W_\pm^-) &= -i \frac{\hat{e}^4}{24 \hat{s}^2 \hat{c}^2} \frac{\hat{S}}{\Lambda^2} \sin \theta \frac{\hat{v}^2}{\Lambda^2} f_{W^2 B \Phi^2}^{(1)}, \\
\mathcal{M}(u_- \bar{u}_+ \rightarrow W_\pm^+ W_\pm^-) &= i \frac{3 \hat{e}^4}{8 \hat{s}^4} \frac{\hat{S}}{\Lambda^2} \sin \theta \left[f_{WWW} + \frac{\hat{v}^2}{2 \Lambda^2} \left(f_{W^3 \Phi^2}^{(1)} - \frac{\hat{s}^2}{18 \hat{c}^2} f_{W^2 B \Phi^2}^{(1)} \right) \right], \tag{4.5}
\end{aligned}$$

as well as

$$\begin{aligned}
\mathcal{M}(d_- \bar{u}_+ \rightarrow Z_\pm W_\pm^-) &= i \frac{3 \hat{c} \hat{e}^4}{4 \sqrt{2} \hat{s}^4} \frac{\hat{S}}{\Lambda^2} \sin \theta \left[f_{WWW} + \frac{\hat{v}^2}{2 \Lambda^2} \left(f_{W^3 \Phi^2}^{(1)} + \frac{\hat{s}^2}{6 \hat{c}^2} f_{W^2 B \Phi^2}^{(1)} \right) \right], \\
\mathcal{M}(d_- \bar{u}_+ \rightarrow Z_0 W_0^-) &= i \frac{\hat{e}^2}{4 \sqrt{2} \hat{s}^2} \frac{\hat{S}}{\Lambda^2} \sin \theta \left(f_W + \frac{\hat{v}^2}{2 \Lambda^2} f_{W \Phi^4 D^2}^{(1)} \right), \\
\mathcal{M}(d_- \bar{u}_+ \rightarrow \gamma_\pm W_\pm^-) &= i \frac{3 \hat{e}^4}{4 \sqrt{2} \hat{s}^3} \frac{\hat{S}}{\Lambda^2} \sin \theta \left[f_{WWW} + \frac{\hat{v}^2}{2 \Lambda^2} \left(f_{W^3 \Phi^2}^{(1)} - \frac{1}{6} f_{W^2 B \Phi^2}^{(1)} \right) \right], \tag{4.6}
\end{aligned}$$

where we indicated the particle polarization as a subscript and we denoted by θ the polar scattering angle in the center-of-mass system. Therefore, the dimension-six-squared contribution to the amplitude squared grows as \hat{S}^2 , while the dimension-eight contribution—which enters in the interference with the SM amplitude—grows as \hat{S} .

Notice that, unlike EWPOs, which correspond to squared amplitudes for fixed center-of-mass energy (either M_Z or M_W), EWDB data correspond to squared amplitudes at different center-of-mass energies. Thus, since at order $1/\Lambda^4$, the dimension-six-squared and the dimension-eight contributions exhibit different energy dependence, the approximate analysis performed in terms of the effective

couplings (4.3), does not exhaust the potential of the data to constrain the Wilson coefficients of all the operators involved. It is then possible to perform an analysis in terms of the seven Wilson coefficients contributing to the amplitudes of the EWDB data because, in fact, to order $1/\Lambda^4$ the χ^2 function depends independently on them,

$$\chi_{\text{EWDB}}^2 \left(f_W, f_B, f_{WWW}, f_{W^2 B \Phi^2}^{(1)}, f_{W \Phi^4 D^2}^{(1)}, f_{B \Phi^4 D^2}^{(1)}, f_{W^3 \Phi^2}^{(1)} \right). \tag{4.7}$$

We present in Fig. 3 the one- and two-dimensional marginalized 68% and 95% C.L. allowed regions for the

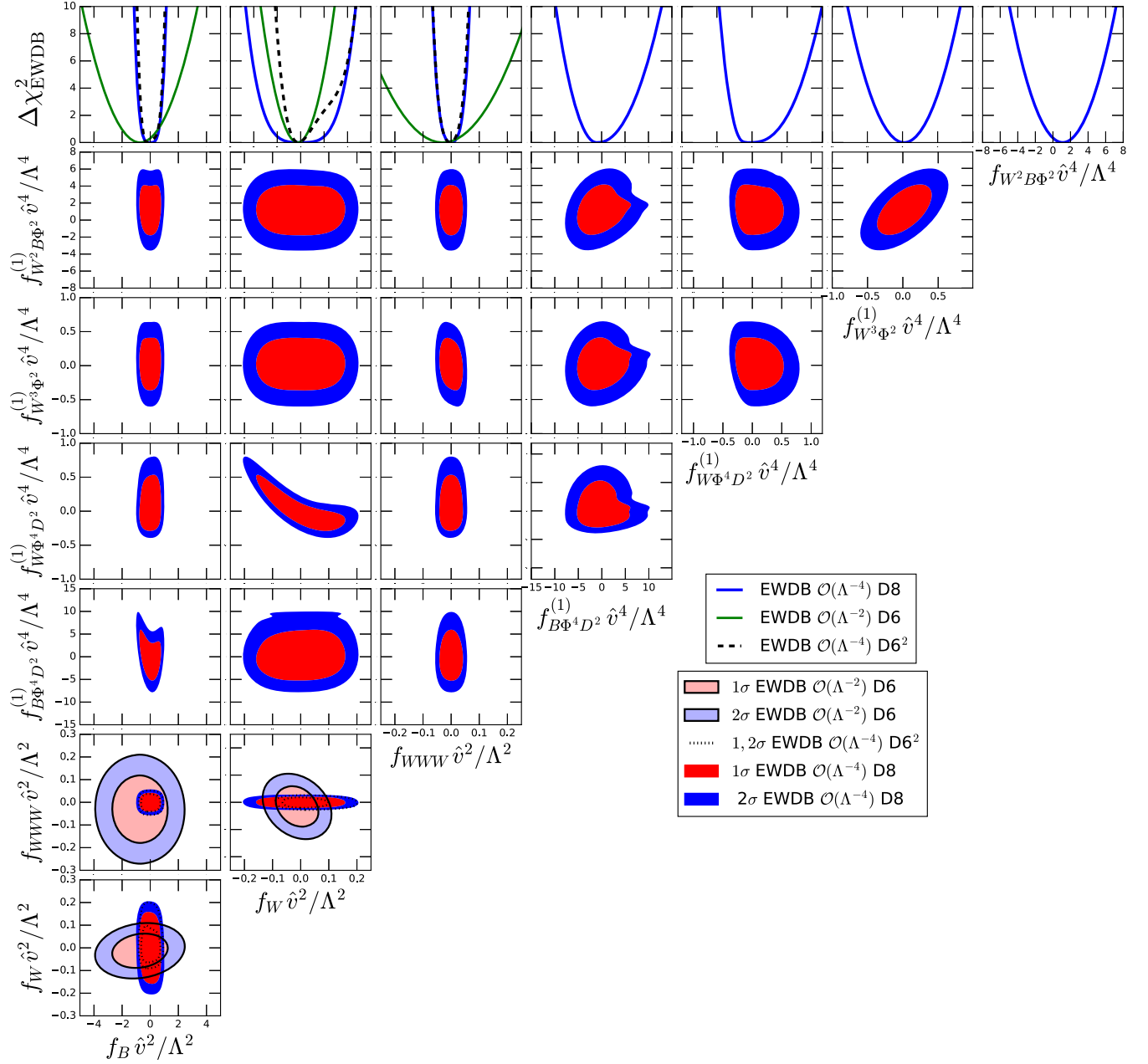


FIG. 3. One- and two-dimensional 68% and 95% C.L. projections of $\Delta\chi^2_{\text{EWDB}}$ for $f_B \hat{v}^2 / \Lambda^2$, $f_W \hat{v}^2 / \Lambda^2$, $f_{WWW} \hat{v}^2 / \Lambda^2$, $f_{B \Phi^4 D^2} \hat{v}^2 / \Lambda^4$, $f_{W \Phi^4 D^2} \hat{v}^2 / \Lambda^4$, $f_{W^3 \Phi^2} \hat{v}^2 / \Lambda^4$, and $f_{W^2 B \Phi^2} \hat{v}^2 / \Lambda^4$ as indicated in the panels after marginalizing over the remaining fit parameters.

seven Wilson coefficients in Eq. (4.7) for several analyses differing by the order in $1/\Lambda$ used in the calculations. We list the corresponding 95% C.L. allowed ranges in Table IV. Notice that the $\mathcal{O}(1/\Lambda^2)$, $[\mathcal{O}(1/\Lambda^4) (\text{dim-6})^2]$ analysis is identical to the one described above as dimension-six $[(\text{dimension-six})^2]$ and leads to the limits on the Wilson coefficients f_W , f_B , and f_{WWW} given in the left (central) column in Table III and the light shaded regions in Fig. 2 (dotted contours) in the three lowest panels. We reproduce these regions and ranges in Fig. 3 and Table IV for clarity and completeness.

From the figure, we see that including the $\mathcal{O}(1/\Lambda^4)$ terms strengthens the constraints obtained at order $1/\Lambda^2$ for the operators \mathcal{O}_B and \mathcal{O}_{WWW} , while it weakens the bounds on \mathcal{O}_W , as expected from the results obtained in the approximate analysis in Fig. 2.

The comparison with the analysis performed including only dimension-six-squared terms in the evaluation of the $1/\Lambda^4$ contribution (see dashed lines) shows that the dimension-six Wilson coefficient, whose determination is most quantitatively affected by the inclusion of the independent effects of the four dimension-eight Wilson

TABLE IV. 95% C.L. allowed range for the Wilson coefficients present in the EWDB data analysis performed with predictions obtained at different orders in the $1/\Lambda^2$ expansion.

Coefficient	EWDB 95% C.L. allowed range		
	$\mathcal{O}(\Lambda^{-2})$	$\mathcal{O}(\Lambda^{-4})$ (dim -6) ²	$\mathcal{O}(\Lambda^{-4})$ (dim -6) ² + dim -8
$\frac{\hat{v}^2}{\Lambda^2} f_B$	[-3.3, 1.8]	[-0.75, 0.83]	[-0.89, 0.89]
$\frac{\hat{v}^2}{\Lambda^2} f_W$	[-0.11, 0.085]	[-0.079, 0.16]	[-0.18, 0.18]
$\frac{\hat{v}^2}{\Lambda^2} f_{WWW}$	[-0.22, 0.16]	[-0.049, 0.045]	[-0.05, 0.05]
$\frac{\hat{v}^4}{\Lambda^4} f_{W^2 B \Phi^2}^{(1)}$			[-2.6, 5.0]
$\frac{\hat{v}^4}{\Lambda^4} f_{B \Phi^4 D^2}$			[-6.48, 7.8]
$\frac{\hat{v}^4}{\Lambda^4} f_{W \Phi^4 D^2}$			[-0.33, 0.66]
$\frac{\hat{v}^4}{\Lambda^4} f_{W^3 \Phi^2}$			[-0.47, 0.51]

coefficients, is f_W . The reason for this is the anticorrelation between f_W and $f_{W \Phi^4 D^2}^{(1)}$ that is apparent in the second panel of the fourth row; see Eq. (4.2). In other words, the EWDB data analyzed provide a weaker discrimination between the dimension-six and the dimension-eight contribution to \tilde{f}_W . On the contrary, the corresponding two-dimensional plots in Fig. 3 show that no large correlations are present between f_B and $f_{B \Phi^4 D^2}^{(1)}$, nor between f_{WWW} and $f_{W^3 \Phi^2}$. The only other large correlation is observed between the dimension-eight coefficients $f_{W^2 B \Phi^2}^{(1)}$ and $f_{W^3 \Phi^2}$ both contributing at the same order to λ_γ and λ_Z . At the linear order on these coefficients, the stronger sensitivity comes from the $W\gamma$ channel, which bounds the combination $6f_{W^3 \Phi^2} - f_{W^2 B \Phi^2}^{(1)}$ [see Eq. (4.2)] leading to the positive correlation observed.

V. SUMMARY AND CONCLUSIONS

We have studied the impact of $\mathcal{O}(1/\Lambda^4)$ corrections in the EWPO and EWDB data analyses assuming a universal C and P conserving new physics scenario. The universality assumption reduces the number of dimension-eight operators contributing to the processes, making a complete analysis possible. As described in Sec. II, in the HISZ basis for the dimension-six SMEFT the universal theories are described by 11 bosonic operators and 5 fermionic operators, the latter being generated by the application of the EOM in the reduction of the basis. At dimension eight, there are ten potentially relevant bosonic operators and one expects a fermionic operator generated by the EOM. Of those, we find that there are six (nine) dimension-six (-eight) operators contributing to the EWPO and EWDB observables [see Eq. (2.9)].

The analysis of EWPOs involves three dimension-six and four dimension-eight operators whose Wilson coefficients cannot be independently bound. However, we find that it is possible to eliminate the blind directions by redefining three effective coefficients, which are just a shift

of the three Wilson coefficients of the dimension-six operators corrected by their corresponding dimension-eight siblings—see Eq. (3.2)—and which contain the sibling dimension-eight contribution to the universal parameters S , T , and δG_F . In addition, the analysis contains a purely dimension-eight contribution to the universal parameter U . The fit to EWPOs performed in terms of these four parameters results in strong constraints on \tilde{f}_{BW} , $\tilde{f}_{\Phi,1}$, $\tilde{\Delta}_{4F}$, and $f_{W^2 \Phi^4}^{(3)}$; see Table I.

At $\mathcal{O}(1/\Lambda^4)$ EWDB analysis involves six (seven) dimension-six (-eight) operators of which three (four) contribute directly to the TGC, while three (three) enter indirectly via the finite renormalization of the SM parameters. The indirect contributions can be cast in terms of three effective couplings bounded by the EWPOs (see Appendix B) allowing us to neglect them in the EWDB analysis. However, this situation will change in the future. As the LHC experiments collect more data, the precision of the EWDB will increase and the indirect contributions will not be negligible anymore. Furthermore, it will also be necessary to take into account the renormalization group evolution (RGE) of the Wilson coefficients since the EWDB and EWPO measurements are not made exactly at the same energy scale. Presently, the RGE effects can be neglected since the difference between the energy scales involved is not large and their numerical value is further suppressed by $1/(16\pi)^2$ factors. Furthermore, taking into account the RGE effects requires performing a global analysis that also includes the Higgs and top data, since the RGE equations introduce dependence on Wilson coefficients of operators contributing to these two sectors [61–64].

The direct contributions to the TGC can be expressed in terms of three effective coefficients that are just a shift of the three Wilson coefficients of the corresponding three dimension-six operators corrected by their corresponding dimension-eight siblings (i.e., rescaled by $\Phi^\dagger \Phi$); see Eq. (4.3). In addition there is a genuine dimension-eight

contribution to the difference between the λ_γ and λ_Z couplings. We performed an effective analysis of the EWDB data in terms of these four coefficients and showed that the bulk of $\mathcal{O}(1/\Lambda^4)$ impact on the analysis is due to the dimension-six-squared contribution $|\mathcal{M}^{(6)}|^2$; see Fig. 2 and Table III. This is so because of the different dependence on the partonic center-of-mass energy of dimension-six-squared terms, which give a pure quadratic TGC contribution to the amplitude squared, and the dimension-eight contribution, which enters in the interference with the SM amplitude.

Profiting from the different energy dependence of the dimension-six-squared and the dimension-eight contributions, it is possible to perform an analysis of the EWDB data, which allows us to constrain the seven Wilson coefficients independently. The result of this analysis is presented in Fig. 3 and Table IV. The results show that the bounds on the three Wilson coefficients of the dimension-six operators are only slightly looser than in the effective four-parameter analysis, while the bounds on the four Wilson coefficients of the dimension-eight operators are all of similar order and all substantially weaker than those on their dimension-six siblings.

In summary, we have shown that, for the universal scenario, the analysis of the EWPO and the EWDB data allows us to constrain the full parameter space of operators up to $\mathcal{O}(\Lambda^{-4})$. Within the present precision of EWDB data and with our choice of basis, it is still consistent to perform the analysis sequentially: first, obtain the constraints on the relevant Wilson coefficients using the EWPOs and then apply those bounds to reduce the number of Wilson coefficients that are relevant for the diboson analysis. That said, the LHC continues to accumulate data on EWDB production, and consequently, we anticipate stronger bounds on the TGCs couplings in the future. At some point, it will be necessary to perform a combined analysis of EWPO + EWDB data taking into account the indirect contributions due to the finite renormalization to the TGCs in analogy with the study TGCs and possible anomalous fermionic couplings [65].

ACKNOWLEDGMENTS

O. J. P. E. is thankful for the hospitality of the Departament de Física Quàntica i Astrofísica, Universitat de Barcelona, where part of this work was carried out. O. J. P. E. is partially supported by CNPq Grant No. 305762/2019-2 and FAPESP Grants No. 2019/04837-9 and No. 2022/05332-0. M. M. is supported by FAPESP Grant No. 2021/08669-3, while P. R. acknowledges support by FAPESP Grants No. 2020/10004-7 and No. 2021/12305-7. This project is funded by USA-NSF Grant No. PHY-1915093. It has also received support from the European Union's Horizon 2020 research and innovation program under the Marie Skłodowska-Curie Grant Agreement No. 860881-HIDDeN and the Horizon Europe research and innovation program under the Marie Skłodowska-Curie Staff Exchange Grant Agreement No. 101086085—ASYMMETRY. It also receives support from Grant No. PID2019-105614 GB-C21, "Unit of Excellence Maria de Maeztu 2020-2023" award to the ICC-UB CEX2019-000918-M, funded by MCIN/AEI/10.13039/501100011033, and from Grant No. 2021-SGR-249 (Generalitat de Catalunya). This manuscript has been coauthored by employees of Fermi Research Alliance, LLC under Contract No. DE-AC02-07CH11359 with the U.S. Department of Energy, Office of High Energy Physics.

APPENDIX A: CORRECTIONS TO THE Z AND W COUPLINGS

We parametrize the Z coupling to fermion (f) pairs as

$$\frac{\hat{e}}{\hat{s}\hat{c}}(\hat{g}^f(1 + \Delta g_1) + Q^f \Delta g_2), \quad (\text{A1})$$

where $\hat{g}^f = T_3^f - \hat{s}^2 Q^f$, T_3^f is the fermion third component of isospin, and Q^f is its charge. After the renormalization of the SM parameters, we obtain at order $1/\Lambda^4$,

$$\begin{aligned} \Delta g_1 &= -\frac{1}{4} \frac{\hat{v}^2}{\Lambda^2} \left[2 \left(\Delta_{4F} + \frac{\hat{v}^2}{\Lambda^2} \Delta_{4F}^{(8)} \right) + f_{\Phi,1} + \frac{\hat{v}^2}{\Lambda^2} f_{D^2\Phi^6}^{(2)} \right] - \frac{1}{32} \frac{\hat{v}^4}{\Lambda^4} [-12(\Delta_{4F})^2 + 4\Delta_{4F}f_{\Phi,1} - 3(f_{\Phi,1})^2] \\ &\simeq -\frac{1}{4} \frac{\hat{v}^2}{\Lambda^2} [2\tilde{\Delta}_{4F} + \tilde{f}_{\Phi,1}] - \frac{1}{32} \frac{\hat{v}^4}{\Lambda^4} [-12(\tilde{\Delta}_{4F})^2 + 4\tilde{\Delta}_{4F}\tilde{f}_{\Phi,1} - 3(\tilde{f}_{\Phi,1})^2]. \end{aligned} \quad (\text{A2})$$

In the last line, we have used that to order $1/\Lambda^4$ the corrections linear in the Wilson coefficients depend on the four combinations in Eq. (3.2); therefore, neglecting terms of $\mathcal{O}(1/\Lambda^6)$, we can rewrite Δg_1 in terms of those combinations. In the same way, we find

$$\begin{aligned} \Delta g_2 &= \frac{\hat{v}^2}{\Lambda^2} \frac{1}{2\hat{c}_2} \left[-\hat{s}^2 \hat{c}^2 (2\tilde{\Delta}_{4F} + \tilde{f}_{\Phi,1}) + \frac{\hat{e}^2}{2} \tilde{f}_{BW} \right] + \frac{\hat{v}^4}{\Lambda^4} \frac{1}{8\hat{c}_2^3} \left\{ \frac{\hat{s}_2^2}{4} \left[(1 + 3\hat{c}_4) \left((\tilde{\Delta}_{4F})^2 + \frac{1}{4} (\tilde{f}_{\Phi,1})^2 \right) - (3 + \hat{c}_4) \tilde{\Delta}_{4F} \tilde{f}_{\Phi,1} \right] \right. \\ &\quad \left. - \frac{\hat{e}^2}{2} (\hat{c}_4 \tilde{f}_{BW} \tilde{f}_{\Phi,1} - 2\tilde{\Delta}_{4F} \tilde{f}_{BW} + \hat{e}^2 (\tilde{f}_{BW})^2) \right\}, \end{aligned} \quad (\text{A3})$$

with $\hat{c}_n = \cos(n\hat{\theta})$ and $\hat{s}_n = \sin(n\hat{\theta})$.

As for the W observables,

$$\begin{aligned} \frac{\Delta M_W}{\hat{M}_W} = & \frac{1}{4\hat{c}_2} \frac{\hat{v}^2}{\Lambda^2} [\hat{e}^2 \tilde{f}_{BW} - 2\hat{s}^2 \tilde{\Delta}_{4F} - \hat{c}^2 \tilde{f}_{\Phi,1}] + \frac{\hat{e}^2}{8\hat{s}^2} \frac{\hat{v}^4}{\Lambda^4} f_{W^2\Phi^4}^{(3)} \\ & + \frac{1}{8\hat{c}_2^3} \frac{\hat{v}^4}{\Lambda^4} \left[-\hat{s}^4 (2 + 3\hat{c}_2) (\tilde{\Delta}_{4F})^2 + \frac{1}{4} \hat{c}^4 (-2 + 5\hat{c}_2) (\tilde{f}_{\Phi,1})^2 - \frac{1}{16} \hat{e}^4 \frac{(7 - 6\hat{c}_2 + 3\hat{c}_4)}{\hat{s}^2} (\tilde{f}_{BW})^2 \right. \\ & \left. - \frac{\hat{c}^2}{4} (9 - 6\hat{c}_2 + 5\hat{c}_4) \tilde{\Delta}_{4F} \tilde{f}_{\Phi,1} + \frac{1}{4} \hat{e}^2 (7 - 2\hat{c}_2 + 3\hat{c}_4) \tilde{\Delta}_{4F} \tilde{f}_{BW} - \frac{1}{2} \hat{e}^2 \hat{c}^2 (-2 + 3\hat{c}_2) \tilde{f}_{\Phi,1} \tilde{f}_{BW} \right], \end{aligned} \quad (\text{A4})$$

where $\hat{M}_W = \frac{\hat{e} \hat{v}}{2\hat{s}}$. And we parametrize the W coupling to left-handed fermions as

$$\frac{\hat{e}}{\hat{s}} (1 + \Delta g_W), \quad (\text{A5})$$

where

$$\begin{aligned} \Delta g_W = & \frac{1}{4\hat{c}_2} \frac{\hat{v}^2}{\Lambda^2} [\hat{e}^2 \tilde{f}_{BW} - 2\hat{c}^2 \tilde{\Delta}_{4F} - \hat{c}^2 \tilde{f}_{\Phi,1}] + \frac{1}{8\hat{c}_2^3} \frac{\hat{v}^4}{\Lambda^4} \left[\hat{e}^2 \frac{\hat{c}_2^3}{\hat{s}^2} f_{W^2\Phi^4}^{(3)} + \hat{c}^4 (-2 + 5\hat{c}_2) (\tilde{\Delta}_{4F})^2 - \frac{1}{16} \frac{(7 - 6\hat{c}_2 + 3\hat{c}_4)}{\hat{s}^2} \hat{e}^4 (\tilde{f}_{BW})^2 \right. \\ & + \frac{1}{4} \hat{c}^4 (-2 + 5\hat{c}_2) (\tilde{f}_{\Phi,1})^2 - \frac{1}{4} \hat{c}^2 (7 - 6\hat{c}_2 + 3\hat{c}_4) \tilde{\Delta}_{4F} \tilde{f}_{\Phi,1} + \frac{1}{4} \hat{e}^2 (5 - 2\hat{c}_2 + \hat{c}_4) \tilde{\Delta}_{4F} \tilde{f}_{BW} \\ & \left. - \frac{1}{2} \hat{e}^2 \hat{c}^2 (-2 + 3\hat{c}_2) \tilde{f}_{\Phi,1} \tilde{f}_{BW} \right]. \end{aligned} \quad (\text{A6})$$

APPENDIX B: CORRECTIONS TO TGC

The renormalization of the SM parameters give rise to indirect contributions to TGC in addition to the direct contributions from the dimension-six and -eight operators to the TGC. Using the parametrization for the $\gamma W^+ W^-$ and $Z W^+ W^-$ TGC given in Eq. (4.1), we find that up to order $1/\Lambda^4$ [and neglecting terms of $\mathcal{O}(1/\Lambda^6)$] the coupling to $W_{\mu\nu}^+ W^{-\mu} Z^\nu$ reads

$$\begin{aligned} g_1^Z = & 1 + \frac{1}{2} \frac{\hat{v}^2}{\Lambda^2} \left[\frac{\hat{e}^2}{4\hat{s}^2 \hat{c}^2} \left(f_W + \frac{\hat{v}^2}{2\Lambda^2} f_{W\Phi^4 D^2}^{(1)} \right) - \frac{1}{\hat{c}_2} \tilde{\Delta}_{4F} + \frac{1}{2} \frac{\hat{e}^2}{\hat{c}^2 \hat{c}_2} \tilde{f}_{BW} - \frac{1}{2\hat{c}_2} \tilde{f}_{\Phi,1} \right] \\ & + \frac{1}{16\hat{c}_2^3} \frac{\hat{v}^4}{\Lambda^4} \left[(1 + 2\hat{c}_2 + 3\hat{c}_4) ((\tilde{\Delta}_{4F})^2 + \frac{1}{4} (\tilde{f}_{\Phi,1})^2) - \frac{\hat{e}^4}{\hat{c}^2} (\tilde{f}_{BW})^2 + 2 \frac{\hat{e}^2}{\hat{c}^2} \tilde{\Delta}_{4F} \tilde{f}_{BW} - (3 - 2\hat{c}_2 + \hat{c}_4) \tilde{\Delta}_{4F} \tilde{f}_{\Phi,1} \right. \\ & \left. - \hat{e}^2 \frac{\hat{c}_4}{\hat{c}^2} \tilde{f}_{BW} \tilde{f}_{\Phi,1} \right] - \frac{\hat{e}^2}{4\hat{s} \hat{c} \hat{s}_4} \frac{\hat{v}^4}{\Lambda^4} \left(\tilde{\Delta}_{4F} - \hat{e}^2 \tilde{f}_{BW} + \frac{1}{2} (1 + 2\hat{c}_2) \tilde{f}_{\Phi,1} \right) f_W, \end{aligned} \quad (\text{B1})$$

The couplings to $W_\mu^+ W_\nu^- V^{\mu\nu}$ are, respectively,

$$\begin{aligned} \kappa_\gamma = & 1 + \frac{1}{8} \frac{\hat{e}^2}{\hat{s}^2} \frac{\hat{v}^2}{\Lambda^2} \left[\left(f_B + \frac{\hat{v}^2}{2\Lambda^2} f_{B\Phi^4 D^2}^{(1)} \right) + \left(f_W + \frac{\hat{v}^2}{2\Lambda^2} f_{W\Phi^4 D^2}^{(1)} \right) - 2\tilde{f}_{BW} \right] \\ & - \frac{\hat{e}^2}{32\Lambda^4} \frac{\hat{v}^4}{\hat{s}^2 \hat{c}_2} (2(1 - \hat{c}_2) \tilde{\Delta}_{4F} - 2\hat{e}^2 \tilde{f}_{BW} + (1 + \hat{c}_2) \tilde{f}_{\Phi,1}) (f_B + f_W - 2\tilde{f}_{BW}) + \frac{\hat{e}^2}{4\hat{s}^2} \frac{\hat{v}^4}{\Lambda^4} f_{W^2\Phi^4}^{(3)} \end{aligned} \quad (\text{B2})$$

and

$$\begin{aligned}
\kappa_Z = 1 &+ \frac{1}{8} \frac{\hat{e}^2}{\hat{s}^2} \frac{\hat{v}^2}{\Lambda^2} \left[\left(f_W + \frac{\hat{v}^2}{2\Lambda^2} f_{W\Phi^4 D^2}^{(1)} \right) - \frac{\hat{s}^2}{\hat{c}^2} \left(f_B + \frac{\hat{v}^2}{2\Lambda^2} f_{B\Phi^4 D^2}^{(1)} \right) + \frac{4\hat{s}^2}{\hat{c}^2} \tilde{f}_{BW} - \frac{4\hat{s}^2}{\hat{e}^2 \hat{c}^2} \tilde{\Delta}_{4F} - \frac{2\hat{s}^2}{\hat{e}^2 \hat{c}^2} \tilde{f}_{\Phi,1} \right] \\
&+ \frac{1}{16\hat{s}^2 \hat{c}^3} \frac{\hat{v}^4}{\Lambda^4} \left[\hat{s}^2 (1 + 2\hat{c}_2 + 3\hat{c}_4) \left((\tilde{\Delta}_{4F})^2 + \frac{1}{4} (\tilde{f}_{\Phi,1})^2 \right) - \hat{e}^4 (2 - 2\hat{c}_2 + \hat{c}_4) (\tilde{f}_{BW})^2 \right. \\
&+ \hat{s}^2 (3 - 2\hat{c}_2 + \hat{c}_4) (2\hat{e}^2 \tilde{\Delta}_{4F} \tilde{f}_{BW} - \tilde{\Delta}_{4F} \tilde{f}_{\Phi,1}) - \hat{e}^2 \hat{s}^2 (-1 + 2\hat{c}_2 + \hat{c}_4) \tilde{f}_{BW} \tilde{f}_{\Phi,1} \\
&+ f_W \left(\hat{e}^2 \hat{c}_2^2 (-2 + \hat{c}_2) \tilde{\Delta}_{4F} + \hat{e}^2 \frac{\hat{c}_2^2}{2} (2 + \hat{c}_2) \left(\frac{\hat{e}^2}{\hat{c}^2} \tilde{f}_{BW} - \tilde{f}_{\Phi,1} \right) \right) \\
&\left. + f_B \hat{e}^2 \frac{\hat{s}^2 \hat{c}_2^3}{2\hat{c}^2} \left(\tilde{f}_{\Phi,1} - 2\tilde{\Delta}_{4F} + \frac{\hat{e}^2}{\hat{s}^2} \tilde{f}_{BW} \right) + 4\hat{e}^2 \hat{c}_2^3 f_{W^2\Phi^4}^{(3)} \right], \tag{B3}
\end{aligned}$$

and the couplings to $W_{\mu\nu}^+ W^{-\nu\rho} V_\rho^\mu$ are

$$\begin{aligned}
\lambda_\gamma &= \frac{3}{2} \frac{\hat{e}^2}{\hat{s}^2} \frac{\hat{M}_W^2}{\Lambda^2} \left[\left(f_{WWW} + \frac{\hat{v}^2}{2\Lambda^2} f_{W^3\Phi^2}^{(1)} \right) + \frac{1}{2\hat{c}_2} \frac{\hat{v}^2}{\Lambda^2} f_{WWW} (\hat{e}^2 \tilde{f}_{BW} - (2\tilde{\Delta}_{4F} + \tilde{f}_{\Phi,1}) \hat{c}^2) \right] - \frac{\hat{M}_W^4}{2\Lambda^4} f_{W^2B\Phi^2}^{(1)}, \\
\lambda_Z &= \frac{3}{2} \frac{\hat{e}^2}{\hat{s}^2} \frac{\hat{M}_W^2}{\Lambda^2} \left[\left(f_{WWW} + \frac{\hat{v}^2}{2\Lambda^2} f_{W^3\Phi^2}^{(1)} \right) - \frac{\hat{v}^2}{\Lambda^2} \frac{\hat{s}^2 (2 + \hat{c}_2)}{\hat{s}_2 \hat{s}_4} f_{WWW} (4\tilde{\Delta}_{4F} \hat{c}^2 + 2\tilde{f}_{\Phi,1} \hat{c}^2 - 2\hat{e}^2 \tilde{f}_{BW}) \right] + \frac{\hat{M}_W^4}{2\Lambda^4} \frac{\hat{s}^2}{\hat{c}^2} f_{W^2B\Phi^2}^{(1)}, \tag{B4}
\end{aligned}$$

where $\hat{M}_W = \hat{e} \hat{v} / 2\hat{s}$.

-
- [1] S. Weinberg, *Physica (Amsterdam)* **96A**, 327 (1979).
[2] H. Georgi, *Weak Interactions and Modern Particle Theory* (Benjamin/Cummings, Menlo Park, CA, 1984), ISBN 9780805331639.
[3] J. F. Donoghue, E. Golowich, and B. R. Holstein, *Dynamics of the Standard Model* (Cambridge University Press, Cambridge, England, 2014).
[4] G. Aad *et al.* (ATLAS Collaboration), *Phys. Lett. B* **716**, 1 (2012).
[5] S. Chatrchyan *et al.* (CMS Collaboration), *Phys. Lett. B* **716**, 30 (2012).
[6] T. Corbett, O. J. P. Éboli, J. González-Fraile, and M. C. González-García, *Phys. Rev. D* **86**, 075013 (2012).
[7] T. Corbett, O. J. P. Éboli, J. González-Fraile, and M. C. González-García, *Phys. Rev. D* **87**, 015022 (2013).
[8] J. Ellis, V. Sanz, and T. You, *J. High Energy Phys.* **03** (2015) 157.
[9] T. Corbett, O. J. P. Éboli, D. Gonçalves, J. González-Fraile, T. Plehn, and M. Rauch, *J. High Energy Phys.* **08** (2015) 156.
[10] A. Butter, O. J. P. Éboli, J. Gonzalez-Fraile, M. C. Gonzalez-Garcia, T. Plehn, and M. Rauch, *J. High Energy Phys.* **07** (2016) 152.
[11] J. Baglio, S. Dawson, and I. M. Lewis, *Phys. Rev. D* **96**, 073003 (2017).
[12] D. Barducci *et al.*, [arXiv:1802.07237](https://arxiv.org/abs/1802.07237).
[13] J. Ellis, C. W. Murphy, V. Sanz, and T. You, *J. High Energy Phys.* **06** (2018) 146.
[14] E. da Silva Almeida, A. Alves, N. Rosa Agostinho, O. J. P. Éboli, and M. C. Gonzalez-Garcia, *Phys. Rev. D* **99**, 033001 (2019).
[15] I. Brivio, S. Bruggisser, F. Maltoni, R. Moutafis, T. Plehn, E. Vryonidou, S. Westhoff, and C. Zhang, *J. High Energy Phys.* **02** (2020) 131.
[16] J. Ellis, M. Madigan, K. Mimasu, V. Sanz, and T. You, *J. High Energy Phys.* **04** (2021) 279.
[17] S. Dawson, S. Homiller, and S. D. Lane, *Phys. Rev. D* **102**, 055012 (2020).
[18] J. J. Ethier, G. Magni, F. Maltoni, L. Mantani, E. R. Nocera, J. Rojo, E. Slade, E. Vryonidou, and C. Zhang, *J. High Energy Phys.* **11** (2021) 089.
[19] E. d. S. Almeida, A. Alves, O. J. P. Éboli, and M. C. Gonzalez-Garcia, *Phys. Rev. D* **105**, 013006 (2022).
[20] B. Henning, X. Lu, T. Melia, and H. Murayama, *J. High Energy Phys.* **08** (2017) 016; **09** (2019) 19.
[21] S. Alioli, R. Boughezal, E. Mereghetti, and F. Petriello, *Phys. Lett. B* **809**, 135703 (2020).
[22] R. Boughezal, E. Mereghetti, and F. Petriello, *Phys. Rev. D* **104**, 095022 (2021).
[23] R. Boughezal, Y. Huang, and F. Petriello, *Phys. Rev. D* **106**, 036020 (2022).
[24] T. Kim and A. Martin, *J. High Energy Phys.* **09** (2022) 124.
[25] L. Allwicher, D. A. Faroughy, F. Jaffredo, O. Sumensari, and F. Wilsch, *J. High Energy Phys.* **03** (2023) 064.
[26] S. Dawson, S. Homiller, and M. Sullivan, *Phys. Rev. D* **104**, 115013 (2021).
[27] C. Degrande and H.-L. Li, [arXiv:2303.10493](https://arxiv.org/abs/2303.10493).
[28] C. Hays, A. Martin, V. Sanz, and J. Setford, *J. High Energy Phys.* **02** (2019) 123.
[29] T. Corbett, A. Martin, and M. Trott, *J. High Energy Phys.* **12** (2021) 147.

- [30] A. Martin and M. Trott, *Phys. Rev. D* **105**, 076004 (2022).
- [31] T. Corbett, *SciPost Phys.* **11**, 097 (2021).
- [32] C. Hays, A. Helset, A. Martin, and M. Trott, *J. High Energy Phys.* **11** (2020) 087.
- [33] T. Corbett, A. Helset, A. Martin, and M. Trott, *J. High Energy Phys.* **06** (2021) 076.
- [34] C. W. Murphy, *J. High Energy Phys.* **10** (2020) 174.
- [35] H.-L. Li, Z. Ren, J. Shu, M.-L. Xiao, J.-H. Yu, and Y.-H. Zheng, *Phys. Rev. D* **104**, 015026 (2021).
- [36] J. D. Wells and Z. Zhang, *J. High Energy Phys.* **01** (2016) 123.
- [37] K. Hagiwara, S. Ishihara, R. Szalapski, and D. Zeppenfeld, *Phys. Rev. D* **48**, 2182 (1993).
- [38] K. Hagiwara, T. Hatsukano, S. Ishihara, and R. Szalapski, *Nucl. Phys.* **B496**, 66 (1997).
- [39] G. F. Giudice, C. Grojean, A. Pomarol, and R. Rattazzi, *J. High Energy Phys.* **06** (2007) 045.
- [40] S. Schael *et al.* (DELPHI, ALEPH, SLD, OPAL, L3 Collaborations, SLD Electroweak Group, SLD Heavy Flavour Group, LEP Electroweak Working Group), *Phys. Rep.* **427**, 257 (2006).
- [41] C. Patrignani *et al.* (Particle Data Group), *Chin. Phys. C* **40**, 100001 (2016).
- [42] T. Aaltonen *et al.* (CDF Collaboration), *Science* **376**, 170 (2022).
- [43] L. E. W. Group (Tevatron Electroweak Working Group, SLD Electroweak and Heavy Flavour Groups, LEP Electroweak Working Group, ALEPH, CDF, DELPHI, SLD, OPAL, D0, L3 Collaborations), *arXiv:1012.2367*.
- [44] J. de Blas, M. Pierini, L. Reina, and L. Silvestrini, *Phys. Rev. Lett.* **129**, 271801 (2022).
- [45] A. Helset, A. Martin, and M. Trott, *J. High Energy Phys.* **03** (2020) 163.
- [46] M. E. Peskin and T. Takeuchi, *Phys. Rev. Lett.* **65**, 964 (1990).
- [47] M. Aaboud *et al.* (ATLAS Collaboration), *Eur. Phys. J. C* **78**, 24 (2018).
- [48] A. Tumasyan *et al.* (CMS Collaboration), *J. High Energy Phys.* **07** (2022) 032.
- [49] A. M. Sirunyan *et al.* (CMS Collaboration), *Phys. Rev. D* **102**, 092001 (2020).
- [50] A. Tumasyan *et al.* (CMS Collaboration), *Phys. Rev. D* **105**, 052003 (2022).
- [51] ATLAS Collaboration, Report No. ATLAS-CONF-2018-034, 2018, <https://cds.cern.ch/record/2630187>.
- [52] G. Aad *et al.* (ATLAS Collaboration), *Eur. Phys. J. C* **81**, 163 (2021).
- [53] G. Aad *et al.* (ATLAS Collaboration), *J. High Energy Phys.* **06** (2021) 003.
- [54] R. Frederix, S. Frixione, V. Hirschi, D. Pagani, H. S. Shao, and M. Zaro, *J. High Energy Phys.* **07** (2018) 185.
- [55] N. D. Christensen and C. Duhr, *Comput. Phys. Commun.* **180**, 1614 (2009).
- [56] A. Alloul, N. D. Christensen, C. Degrande, C. Duhr, and B. Fuks, *Comput. Phys. Commun.* **185**, 2250 (2014).
- [57] T. Sjostrand, S. Mrenna, and P. Z. Skands, *Comput. Phys. Commun.* **178**, 852 (2008).
- [58] J. de Favereau, C. Delaere, P. Demin, A. Giammanco, V. Lemaitre, A. Mertens, and M. Selvaggi (DELPHES 3 Collaboration), *J. High Energy Phys.* **02** (2014) 057.
- [59] M. Cacciari, G. P. Salam, and G. Soyez, *Eur. Phys. J. C* **72**, 1896 (2012).
- [60] K. Hagiwara, R. D. Peccei, D. Zeppenfeld, and K. Hikasa, *Nucl. Phys.* **B282**, 253 (1987).
- [61] E. E. Jenkins, A. V. Manohar, and M. Trott, *J. High Energy Phys.* **10** (2013) 087.
- [62] E. E. Jenkins, A. V. Manohar, and M. Trott, *J. High Energy Phys.* **01** (2014) 035.
- [63] R. Alonso, E. E. Jenkins, A. V. Manohar, and M. Trott, *J. High Energy Phys.* **04** (2014) 159.
- [64] A. Helset, E. E. Jenkins, and A. V. Manohar, *J. High Energy Phys.* **02** (2023) 063.
- [65] A. Alves, N. Rosa-Agostinho, O. J. P. Éboli, and M. C. Gonzalez-Garcia, *Phys. Rev. D* **98**, 013006 (2018).